Adsorption 11: 169–172, 2005

Structural Study of $CHCl_3$ Molecular Assemblies in Micropores Using X-ray Techniques

TAKU IIYAMA* AND YOSHIE KOBAYASHI
Department of Chemistry, Faculty of Science, Shinshu University, 3-1-1 Asahi, Matsumoto 390-8621, Japan
tiiyama@shinshu-u.ac.jp

ATSUSHI MATSUMOTO AND YOSHITAKA NAKAHIGASHI
Ad'all Co., Ltd., 5 Tonouchi, Uji, Kyoto 611-8555, Japan
nakahigashi@adall.co.jp

SUMIO OZEKI
Department of Chemistry, Faculty of Science, Shinshu University, 3-1-1 Asahi, Matsumoto 390-8621, Japan
sozeki@shinshu-u.ac.jp

Abstract. The X-ray diffraction from $CHCl_3$ molecules adsorbed in slit-shaped micropores of activated carbon fibers were measured at 298 K. The pore effect on structure of molecular assemblies in the graphitic micropores was examined. The peak positions due to the first nearest neighbor $CHCl_3$ in the electron radial distribution function of adsorbed phase agreed with those of bulk liquid, although their peak intensities were different. In narrow pores (pore width $w = 1.1$ nm), the peak intensities due to the first nearest molecule are stronger than the bulk liquid, because a peak due to the correlation between carbon walls and $CHCl_3$ molecules was overlapped. In the wider pores of ACF W10 ($w = 1.3$ nm) having high $CHCl_3$ removal efficiency from tap water, the intensity of the peak of $r = 0.4$ nm is the strongest. It suggests that $CHCl_3$ molecules in the 1.3 nm micropores should be orientated for a Cl atom to meet with a carbon atom in wall surfaces. These results demonstrate that the structure of a polar molecule such as $CHCl_3$ will sensitively be subject to micropore effects.

Keywords: $CHCl_3$(chloroform), microporous carbon, XRD, radial distribution function, dipole

1. Introduction

The behavior of molecules confined in small space has attracted much attention. These molecules show the special phenomena such as unique phase transition and ordered structure formation (Iiyama et al., 1997a). One of origins of these phenomena is the fact that the adsorbed phase is constituted by small number of molecules.

The analysis method for adsorbed phases in the micropore in molecular level is limited, because the micropore space is surrounded by the solid. Since X-ray can penetrate various materials, we can detect directly the structural information on adsorbed phase itself in micropore with the X-ray techniques. The information of intermolecular structure among adsorbed molecules can be obtained by *in situ* X-ray diffraction (XRD) measurement. In previous studies, we showed by using this method that water molecules form a solid-like structure in the carbon micropore even at room temperature (Iiyama et al., 1995).

On the other hand, small angle X-ray scattering (SAXS) can provide the information about shape and size of adsorbed molecular assemblies (Iiyama et al.,

---

*To whom correspondence should be addressed.

2000). The density fluctuation of adsorption systems changes with adsorption which molecules fill empty pores. We reported that the density fluctuation and correlation length from SAXS can directly translate to the size of both adsorbed molecular assemblies and vacant (Iiyama et al., 2004).

In this paper, we report adsorption state of $CHCl_3$ in carbon micropore using *in situ* XRD. Filling states of $CHCl_3$ molecules in the micropores are governed by the molecule-surface and intermolecular interactions, which should be quite sensitive to the pore width and shape. The behavior of a polar $CHCl_3$ molecule in the hydrophobic space is interesting from the scientific viewpoint. On the other hand, $CHCl_3$ is a carcinogen, and the removal from tap water is strongly desired. The adsorption method using microporous materials is the most effective method for $CHCl_3$ removal from water containing very small amount (Chang et al., 1997). We try to determine the intermolecular structure of $CHCl_3$ assemblies in the carbon micropore, and the relation of the assembly structure with $CHCl_3$ removal efficiency of activated carbons is discussed.

2. Experimental

Two kinds of pitch-based activated carbon fibers (ACFs; Ad'all Co.), A20 and W10, were used as adsorbents. Two ACF samples have different porosities. W10 has 5 times greater $CHCl_3$ removal efficiency than A20 in the water flow condition. The micropore structures of these samples were determined by N_2 adsorption at 77 K after pre-heating at 383 K and 1 mPa for 2 h. The $CHCl_3$ adsorption isotherms were determined at 298 K by a volumetric method.

The XRD profiles from $CHCl_3$ adsorbed samples at 298 K were measured with the transmission method by use of an angle-dispersion diffractometer (Rigaku, AFC-5R) with Mo K_α radiation. The scattering parameter s ($s = 4\pi \sin\theta/\lambda$, where 2θ and λ are the scattering angle and the wave length of X-ray, respectively) ranging from $s = 7$ to 120 nm^{-1} was covered. The XRD profiles were corrected by an appropriate method, and the scattering intensity from adsorbed $CHCl_3$ assembly was extracted from the XRD profiles corrected by subtraction the diffraction data of carbon itself. The experimental setup and extracting methods were already published in the previous article (Iiyama et al., 1997b).

The electron radial distribution function (ERDF) analysis for the amorphous structure (Warren, 1934) was applied to adsorbed $CHCl_3$ molecular assembly in the micropore. The ERDF, $4\pi r^2(\rho(r)\text{-}\rho_0)$, is obtained by the Fourier transformation of the extracted XRD profiles. Here $\rho(r)$ and ρ_0 are the density at a distance r and the average density, respectively. The ERDF expresses the local molecular structure of adsorbed $CHCl_3$ by the distribution of the electron density.

3. Results and Discussion

N_2 adsorption isotherms at 77 K were of Type I. The micropore volume $W_0(N_2)$ and specific surface areas a_α are shown in Table 1. The external surface area is negligibly small compared with a_α. We assumed the slit-shaped pore because the pore wall had been composed of the graphite crystallite. The average pore widths w estimated from both of a_α and $W_0(N_2)$ are also shown in Table 1. The average pore widths of A20 and W10 correspond to the 1.9 and 2.2 adsorbed layers, respectively.

The adsorption isotherms of $CHCl_3$ on ACF at 298 K are shown in Fig. 1. The ordinate is expressed by the fractional filling of $CHCl_3$, $\phi = v/v_0$, where v and v_0 are volume of adsorbed $CHCl_3$ and that of saturated condition, respectively. They are also Type I.

Table 1. The pore structure of ACF samples by N_2 adsorption at 77 K.

	Micropore volume $W_0(N_2)$/mL g^{-1}	Surface area $a_\alpha/m^2\ g^{-1}$	Pore width w/nm
A20	1.01	1770	1.1
W10	0.50	760	1.3

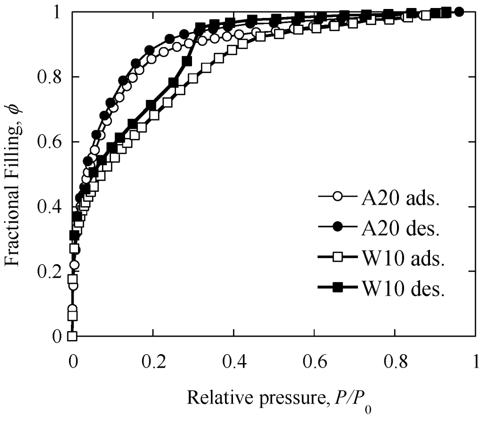

Figure 1. Adsorption isotherms of $CHCl_3$ on ACF samples at 298 K.

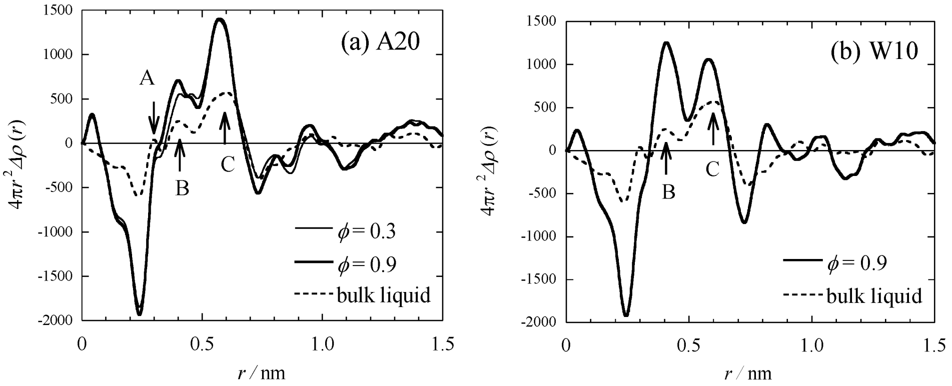

Figure 2. The ERDF of $CHCl_3$ adsorbed in micropores and bulk liquid $CHCl_3$ at 298 K. (a) A20, (b) W10. Broken lines are for bulk liquid of $CHCl_3$.

The initial uptakes in A20 were much greater than W10. The isotherm for W10 showed the significant hysteresis around $P/P_0 = 0.35$, indicating some portion of $CHCl_3$ filled by capillary condensation in mesopores. The micropore volumes from $CHCl_3$ adsorption, $W_0(CHCl_3)$ were estimated using the density of bulk liquid $CHCl_3$ ($\rho_{CHCl_3} = 1.49$ g ml^{-1}). The volume ratio $W_0(CHCl_3)/W_0(N_2)$ of A20 and W10 were 1.05 and 1.15. The positive deviation from unity suggests a dense packing of adsorbed $CHCl_3$ molecules.

Figure 2(a) shows the ERDF of $CHCl_3$ adsorbed in micropores of A20 at 298 K and $\phi = 0.3$ and 0.9. For comparison, the ERDF of bulk liquid $CHCl_3$ is also shown in Fig. 2. The ERDF of bulk $CHCl_3$ shows the characteristic peaks at 0.30 nm (A), 0.40 nm (B), and 0.61 nm (C), which are attributed to, respectively, H — Cl, Cl — Cl (near side), Cl — Cl (far side) distances of the nearest neighbor $CHCl_3$ (Bertagnolli and Chieux, 1980; Bertagnolli, 1981). The peak positions for ERDF of adsorbed state agree with that of bulk liquid, indicating that the adsorbed $CHCl_3$ has a similar structure to bulk liquid. However, the intensities of peaks B and C are much stronger than these of bulk liquid. The strong peaks suggest that an ERDF peak at around 0.3–0.6 nm, which arises from the interference between $CHCl_3$ molecules and carbon wall, should overlap with Cl–Cl peaks. The distance 0.45 nm was the center-to-center distance between an adsorbed $CHCl_3$ molecule and a carbon atom at pore wall, since a $CHCl_3$ molecule is regarded as a sphere of the 0.58 nm diameter (Israelachvili, 1991a). Moreover, decrease in the mobility of $CHCl_3$ adsorbed may cause increase in the amplitude of ERDF. The ERDFs of adsorbed $CHCl_3$ at $\phi = 0.3$ and 0.9 agreed with each other in the whole r range. It is considered that $CHCl_3$ molecule adsorbed in the micropore form cluster-like assembly by lateral interaction between ad-molecules even at low ϕ region.

Figure 2(b) shows the ERDF of $CHCl_3$ adsorbed at $\phi = 0.9$ in the W10 system. The ERDF curve has similar features to the A20 case, but the intensity of peak B is the strongest, different from the A20 system (in which peak C is the strongest). This feature suggests a special orientation of $CHCl_3$ molecule in W10 systems. We estimated the interference term between carbon wall and adsorbed $CHCl_3$ assuming several geometrical arrangements. Figure 3 shows the two configurations of a $CHCl_3$ molecule on a graphite surface: in Model A, three Cl atoms contact with a carbon wall and on Model B, two Cl atoms and an H atom contact with the wall. These configurations may give theoretical interference term in the ERDF (Prins and Peterson, 1936). The both models it is inferred that gave the largest peak at 0.40 nm, but the peak in Model A was larger than that in Model B. Therefore, $CHCl_3$ adsorbed in W10 should be oriented as Model A.

These results show that the structure of adsorbed $CHCl_3$ assemblies sensitively responds to the micropore structure. This seems to originate from the facts that $CHCl_3$ is polar and its diameter close to the pore width. Though $CHCl_3$ is adsorbed by mainly dispersion force with the carbon surface, the structure of adsorbed phase seems to be influenced by the dipole-dipole interaction. The maximum dipole-dipole attraction occurs when two dipoles are lying in line (→→), which is twice as much as while for two dipoles aligned parallel to each other (↑↓) (Israelachvili, 1991b). It is known that the bulk liquid of $CHCl_3$ contains the structure in which the dipoles lying in line (Bertagnolli, 1981). However, in the carbon pores, another structure may be

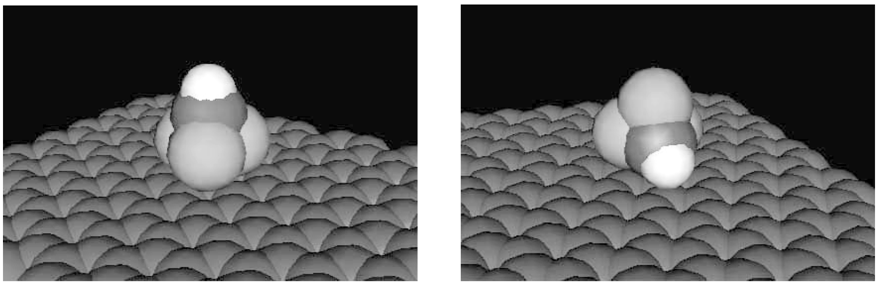

Model A Model B

Figure 3. The configuration models of adsorbed $CHCl_3$.

stabilized, because the micropores can be considered almost two-dimensional space. It was shown by the computer simulation and XRD measurements that in the CCl_4-carbon micropore system the CCl_4 structure sensitively changed with micropore width in the range of 1 to 2 molecular diameters (Iiyama et al., 1997b; Suzuki et al., 1999). In the $CHCl_3$-W10 system, the adsorbed molecules form ordered structure in which the dipole stands in vertical to the carbon surface and an anti-parallel side-by-side order. In this arrangement, the mirror potential should also effectively works (Wang et al., 1995). It is considered that the intermolecular interaction in $CHCl_3$ assemblies in the micropores should lead to the high $CHCl_3$ removal efficiency of W10.

References

Bertagnolli, H. and P. Chieux, *Ber. Bunsenges. Phys. Chem.*, **84**, 1225–1231 (1980).

Bertagnolli, H., *Ber. Bunsenges. Phys. Chem.*, **85**, 644 (1981).

Chang, T.-M., L.X. Dang, and K.A. Peterson, *J. Phys. Chem. B*, **101**, 3413–3419 (1997).

Iiyama, T., K. Nishikawa, T. Otowa, and K. Kaneko, *J. Phys. Chem.*, **99**, 10075–10076 (1995).

Iiyama, T., K. Nishikawa, T. Suzuki, and K. Kaneko, *Chem. Phys. Lett.*, **274**, 152–158 (1997a).

Iiyama, T., K. Nishikawa, T. Suzuki, T. Otowa, M. Hijiriyama, Y. Nojima, and K. Kaneko, *J. Phys. Chem. B*, **101**, 3037–3042 (1997b).

Iiyama, T., M. Ruike, and K. Kaneko, *Chem. Phys. Lett.,* **331**, 359–364 (2000).

Iiyama, T., Y. Kobayashi, K. Kaneko, and S. Ozeki, *J. Coll. Surf. A*, **241**, 207–213 (2004).

Israelachvili, J., *Intermolecular and Surface Forces,* 2nd ed., pp. 109–111, Academic Press, London, 1991a.

Israelachvili, J., *Intermolecular and Surface Forces,* 2nd ed., pp. 57–60, Academic Press, London, 1991b.

Prins, J.A. and H. Petersen, *Physica*, **3**, 147 (1936).

Suzuki, T., T. Iiyama, K.E. Gubbins, and K. Kaneko, *Langmuir*, **15**, 5870–5875 (1999).

Wang, Z.M. and K. Kaneko, *J Phys. Chem.*, **99**, 16714 (1995).

Warren, B.E. and N.S. Gingrich, *Phys. Rev.*, **46** 368 (1934).